



The New Champlain Bridge – Seismic Hazard, Analysis, and Design

Marwan Nader¹, Tim Ingham², Thaleia Travasarou³, Guy Mailhot⁴

¹ Senior Vice President, T.Y. Lin International, San Francisco, CA.

² Vice President, T.Y. Lin International, San Francisco, CA.

³ Manager Land GeoConsulting Americas, Fugro USA Land, Walnut Creek, CA.

⁴ Chief Engineer, Infrastructure Canada, Montreal, QC.

ABSTRACT

The New Champlain Bridge is one of the largest infrastructure projects in North America. It represents a landmark structure which is of critical economic importance to the greater Montreal region and to Canada. The 3.4 km bridge is comprised of three structures: a signature 529 m asymmetric Cable-Stayed Bridge (CBS) with a main span of 240 m; a 762 m East Approach with a maximum span of 109 m; and a 2,044 m West Approach with a typical span of 80.4 m.

The New Champlain Bridge site is within the stable continental interior of the North American Plate. However, this region is seismically active, and several distinct zones of seismicity exist within southeastern Canada. The bridge was designed to meet specified performance criteria for three design levels corresponding to the 475, 975, and 2475-year return periods and is designated as a lifeline structure. Given the level of seismicity of the area, the design of the piers using precast segments and internal post-tensioning, and the requirement that the bridge be repairable following a strong seismic event (2475-yr return period), an essentially elastic design of the bridge for seismic loads was desired. Therefore, structural analysis of the bridge was carried using response spectrum analysis and the factored seismic loads were included in load combinations alongside other design loads. The design of the cable-stayed bridge and the approaches were carried out independently but later reconciled, particularly with respect to displacement demands at expansion joints. The design of the entire bridge—including both approaches and the cable-stayed bridge was subsequently verified using nonlinear time history analysis of a single, comprehensive model.

Keywords: Cable-stayed bridge, seismic hazard, liquefaction, lateral spreading, nonlinear time history analysis.

INTRODUCTION

The existing Champlain Bridge in Montreal, Quebec, Canada, opened to traffic in 1962, is one of the country's busiest crossings. The deteriorating bridge has undergone extensive and costly rehabilitation during its service life. In 2013, the Government of Canada announced that it would replace the bridge under an accelerated schedule. The New Champlain Bridge (now officially named the Samuel De Champlain Bridge) crosses the St. Lawrence River downstream of the old bridge between Île des Sœurs (part of the City of Montreal) and the river's South Shore. The 3.4-kilometre-long signature bridge is the key element of the New Champlain Bridge Corridor Project, which includes nearby highway reconstruction, widening of the federal portion of Autoroute 15, and a new Île des Sœurs Bridge.

Serving as a gateway to Montreal, the New Champlain Bridge comprises three independent superstructures: the 529-metre-long, asymmetric cable-stayed bridge (CSB) signature span, which features a single, 158.6-metre-high tower (measured from the bottom of the footing) and stay cables in an aesthetic harp arrangement; the 762-metre-long East Approach; and 2,044-metre-long West Approach. The bridge elevation is shown in Figure 1.

The three-corridor design includes two four-lane corridors for vehicular traffic, a transit corridor designed to accommodate a light-rail transit system (now underway), and a multi-use path for pedestrians and bicyclists adjacent to the northern highway corridor resulting in an unsymmetrical deck. Along with an aggressive design-build schedule, the project came with stringent design and performance criteria, including notably, modern performance-based seismic design requirements based on North American best practices. Site challenges included severe winter conditions, wind and seismic hazards, strict navigational requirements, and construction in a dense urban setting. An innovative visual quality approach was used to define the bridge's main architectural features and to meet the public's expectations. By utilizing precasting, modular segments with post-tensioning and by developing innovative erection methods and sequencing to their fullest potential, the project team met the accelerated schedule of only 42 months from design to essentially complete in construction, all while meeting the high-

durability performance requirements imposed by the Owner. The New Champlain Bridge is expected to open to traffic summer of 2019. A rendering of the bridge is shown in Figure 2.

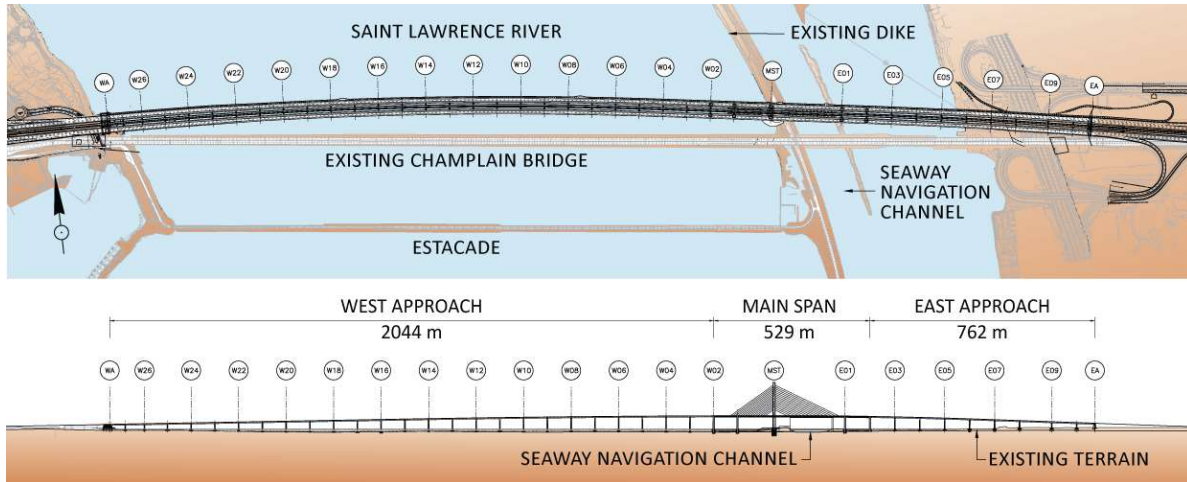


Figure 1, Bridge Plan and Elevation



Figure 2, Bridge Rendering

SEISMIC HAZARD

Design Spectra

The New Champlain Bridge site is within the stable continental interior of the North American Plate. This region is seismically active, and several distinct zones of seismicity exist within southeastern Canada. No evidence exists to associate historical seismicity with active faulting [1]. Given the moderate seismic hazard, design spectra for spectral analyses were developed based on the generic spectral shapes and amplification factors in the Project Agreement (PPP Contract).

Based on historical analysis, within 200 km of Montreal, the associated Magnitudes and probabilities of EQ magnitudes are as follows: 1 in 10,000 event (.0001 per annum): Magnitude 7.0; 1 in 2,500 event (.0004 per annum): Magnitude 6.5 and 1 in 1,000 event (.0010 per annum): Magnitude 6.1.

Overall, the reference rock at the project site, was classified as Site Class B with a time-weighted averaged shear wave velocity (V_{s30}) of approximately 1100 m/s. In areas where the soil overburden exceeded about 5.0 metres the seismic site classification from the as-built ground surface was assigned as Site Class C. These areas include the cable stayed bridge, west abutment, and east approach. Computed peak ground acceleration values for site class B spectra were 0.095, 0.16, and 0.3 for the 475, 975, and 2475-year return periods respectively. Site-specific wave propagation analyses were conducted: a) to develop depth-varying time histories for the cable stayed bridge, and for Frame E2 of the east approach where deep foundations were used, b) to develop near-surface site-specific spectra.

Rock Time Histories Including Wave Passage and Incoherency

Five sets of two-horizontal and one-vertical component time histories were developed for the horizontal and vertical design acceleration response spectra for return periods of 975 and 2475 years. These were used in subsequent site response and nonlinear structural time history analyses. The selection was based on earthquake magnitude and site-to-source distance from seismic hazard deaggregation, spectral shape, peak intensity, and ground motion duration. Seismic hazard deaggregation for structural periods of 1 to 5 seconds are associated with mean earthquake magnitude of 6.7 at mean distances between 50 to 100km. The seed ground motions included simulated time histories for eastern Canada [2], a record from the magnitude 6.8 1985 Nahanni earthquake, and two motions developed for rock conditions in the Central and Eastern United States (CEUS) by REI [3]. Ground motion modification was performed in the time domain by introducing wavelets in the seed time history to adjust its amplitude and frequency content. The seed motions were matched to the target spectra for site class B.

The spatial variation of ground motions associated with wave passage and wave incoherency effects was incorporated in the time histories developed for analyses. The plane-wave coherency model proposed in Abrahamson [4] was extrapolated to distances up to 2,500 metres to cover the range of separation distances of the bridge piers. An example of the set of incoherent motions for all piers is shown in Figure 3 in terms of acceleration, velocity, and displacement time histories and acceleration response spectra. Ground motion incoherency affects mostly the high frequencies.

The wave passage effect was incorporated by applying a systematic time shift in the arrival of the seismic waves at each pier location, which depends on the velocity of the seismic waves along the bridge and the direction of propagation. A rock shear wave velocity equal to 2.5 km/s was used for the calculation of the wave passage effects.

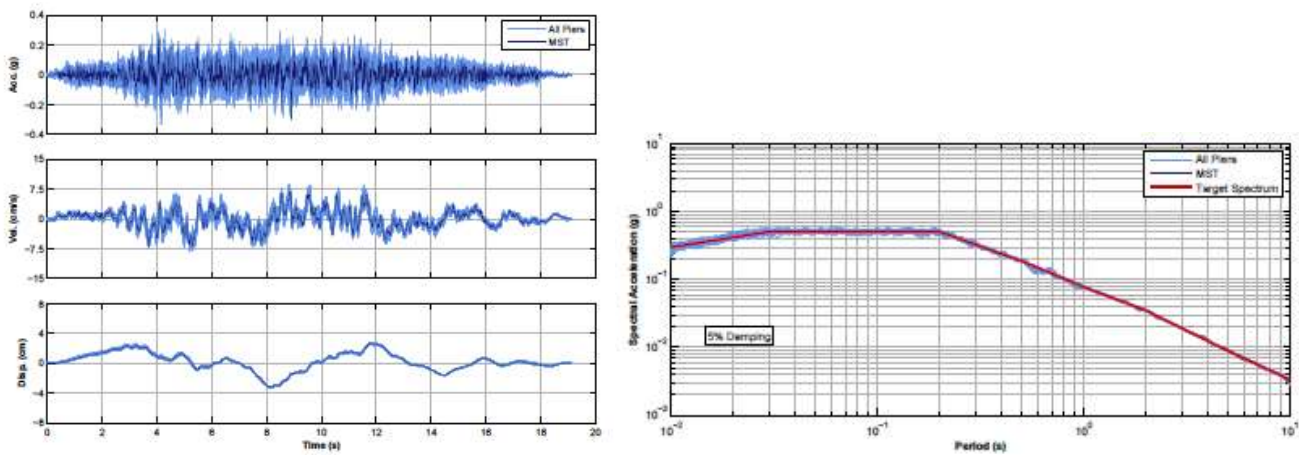


Figure 3, Example of Incoherent Ground Motion Set – Nahanni Mackenzie ST3 Motion – 2475-Year Return Period

GROUND MOTIONS FOR TIME HISTORY ANALYSIS

Depth-varying ground motions were developed at two locations along the cable stayed bridge (MST, E01), and East Approach (i.e., piers E07 to E10 and East Abutment) founded on deep drilled shaft foundations. These motions were developed by conducting one-dimensional (1-D) site response analyses. Due to the liquefaction potential of the existing fill, the site response analyses included two cases considering no liquefaction and liquefaction of the fill. The analyses were performed with the finite difference program FLAC [5] in combination with the Itasca Hysteresis Sigmoidal (S3) Model for non-liquefiable strata and UBCSAND [6] for liquefiable fill. At the MST the stratigraphy comprised approximately 6 metres of fill overlying 2 metres of Glacial Till, over shale rock grading from very poor at a depth of 11 metres to very good at a depth of about 21 metres. The idealized shear wave velocity profile was developed based on site-specific velocity data for rock, and using empirical relationships proposed by Seed and Idriss (1970) based on representative K_{2max} values for the fill and Glacial Till. The overburden soil appears to amplify the input ground motion near the fundamental period of the soil column, which is about 0.26 second. Overall, the input ground motion is not modified for longer periods, i.e., greater than about 1.0 second. The liquefaction case generally results in lower ground surface spectral accelerations, particularly at the fundamental period of the soil column (Figure 4). Based on these results, the overall stronger, no-liquefaction spectra and ground motions were used for design.

Figure 5 compares the site-specific response spectra calculated from similar 1D site response analyses performed for the east approach Frame 2 compared to the generic Site Class C response spectra defined in the Project Agreement (PA). The amplitude of the long period energy for the site-specific response spectra is lower than the amplitudes given by the response spectra from the PA. Conversely, the amplitude of the short period energy is higher for the site-specific response spectra. These comparisons

illustrate the differences between site-specific amplification factors calculated herein and the generic site amplification factors used in the PA. The site-specific spectra developed here for the East Approach were used in design, thus reducing the ground motions at longer periods which are comparable to the structural period of the bridge.

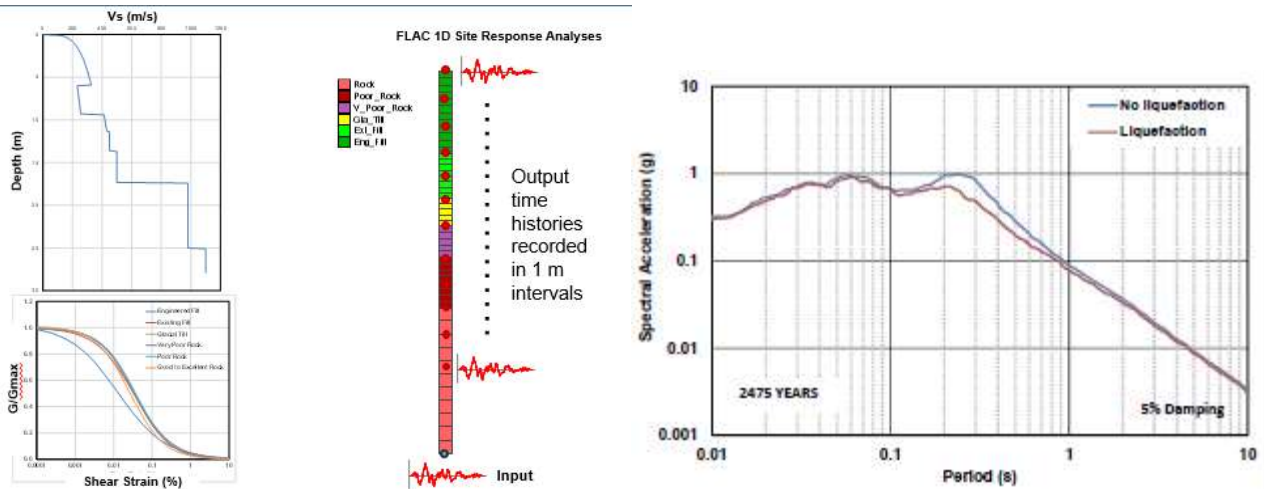


Figure 4, 1D Site Response Analyses for Depth-Varying Ground Motions at the MST

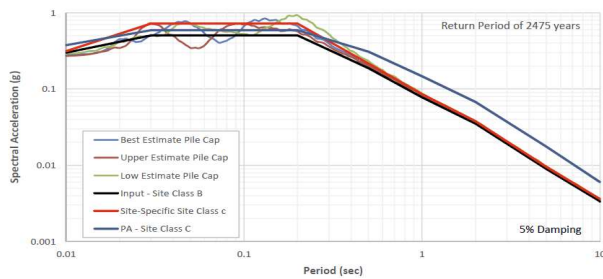


Figure 5, Generic (per PA) vs Site-Specific Acceleration Response Spectra at Pile Cap Elevation for Frame 2 - East Approach

LIQUEFACTION AND LATERAL SPREADING

Qualitative and quantitative assessments of liquefaction susceptibility suggest that the artificial fill, present along much of the bridge, alignment is susceptible to liquefaction if submerged. At the MST and E01, loose liquefiable soil was encountered underneath the proposed permanent berm. This approximately 2 to 3-metre layer may be associated with dike fills placed in a loose condition during dike construction or the St. Lawrence River deposits encountered in the river as suggested by the historic drawings (Figure 6). At the MST and E01, liquefaction triggering is likely under the 2475- and 975-year events; however, widespread liquefaction is unlikely under the 475-year event (10% probability of exceedance in 50 years).

Two-dimensional, nonlinear effective-stress, coupled, dynamic analyses were performed in FLAC [5] to estimate the liquefaction-induced displacement demands adjacent to the MST, E01 and WA. These analyses were performed for the 975- and 2475-year design levels using the five design acceleration time histories. Approximately 30 cm of horizontal displacement was estimated at the MST foundation location during 2475-year return period event (Figure 6). After the end of shaking, the static stability was also assessed using a post-liquefaction residual strength for the liquefied material. The displacement time histories computed from these rigorous numerical analyses, using appropriate liquefaction models for the liquefiable fill, were incorporated in the structural foundation model as excitations, including the effect of liquefaction (Figure 7).

The design team considered two approaches to address the potential for liquefaction-induced demands on the MST, E01 and WA foundations. The first consisted of appropriately designing the affected foundations for liquefaction-induced vertical and horizontal demands. The second considered liquefaction mitigation measures, including partial removal of liquefiable soils. The first approach was selected for final design, to meet the aggressive construction schedule and reduce cost, hence foundations affected by liquefiable soils were designed to withstand liquefaction-induced demands. At MST, the performance criteria of the permanent berm protecting the MST (i.e., regardless of impact on foundation) was also be considered for berm design.

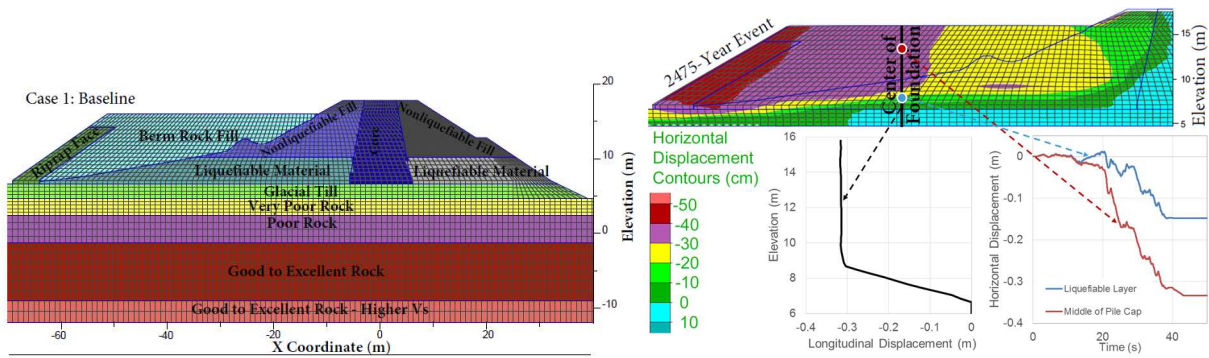


Figure 6, Assessment of Liquefaction-Induced Lateral Spreading near the MST and Permanent Berm.

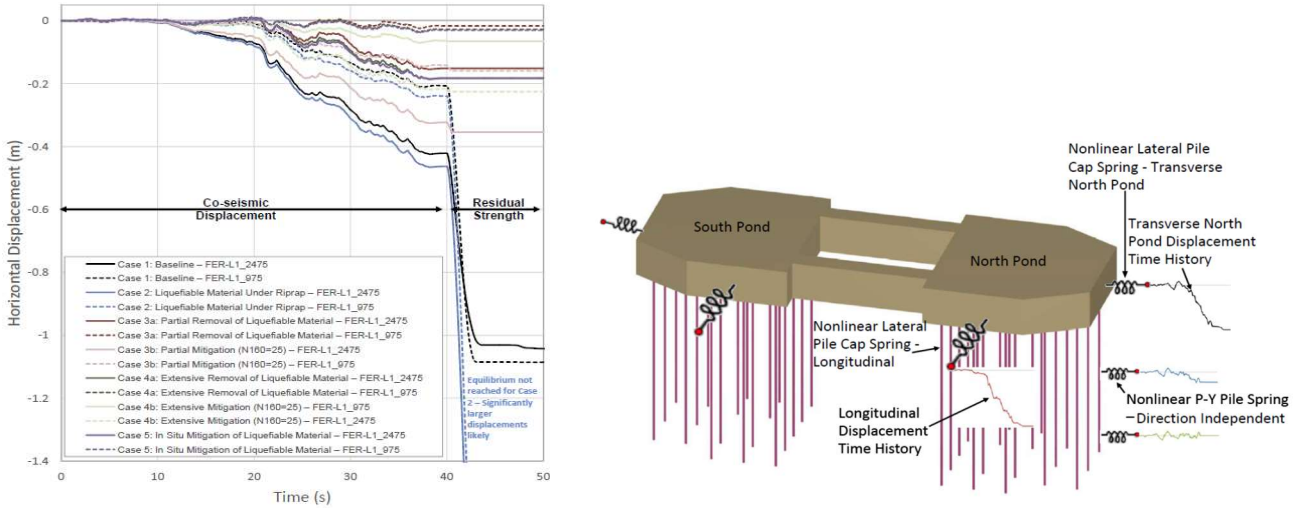


Figure 7, Potential Liquefaction Mitigation Sensitivity Analyses (results shown at middle of riprap) and Approach to Incorporate Depth-Varying Ground Motions, and Nonlinear Soil Springs in Structural Analyses.

RESPONSE SPECTRUM ANALYSIS FOR DESIGN

The seismic design of the New Champlain Bridge was carried out using response spectrum analysis and elastic design, in accordance with the detailed requirements of the Project Agreement [7], the Design Basis Report [8], and an advance draft version of the newer version of Canadian Highway Bridge Design Code intended to replace the existing version of Canadian Highway Bridge Design Code [9]. The bridge was designed as a lifeline bridge. Lifeline bridge, per CHBDC S-14, is described as “A large, unique, iconic, and/or complex structure that is vital to the integrity of the regional transportation network, the ongoing economy, and the security of the region and represents significant investment and would be time-consuming to repair or replace. It is classified as seismic performance category 3.

The seismic design of the bridge was carried out using the essentially elastic design approach permitted under the Project Agreement. By adopting the essentially elastic design approach, the unfactored ultimate resistance of the structures and foundations were provided to exceed the design forces equal to 1.30 times the forces obtained from analysis with seismic ground motions with a probability of exceedance of 2% in 50 years (2475 years return period).

Response spectrum analysis was performed using RM Bridge Advanced V8i.08.11.18.01 [10]. The cable-stayed bridge model used is shown in Figure 8. The model encompasses the cable-stayed bridge from Pier W02 to E02 and the adjacent spans from W03 to W02 and from E02 to E03.

Lateral spreading forces on the main tower foundation of the cable-stayed bridge were addressed by performing two analyses:

- A response spectrum analysis performed with soil springs representing the non-liquefied stiffness of the soil.
- A second analysis performed with soil springs representing the liquefied stiffness of the soil. These dynamic results were combined with the static forces obtained by applying a static lateral spreading force representing the pressure of the liquefied soil on the foundation.

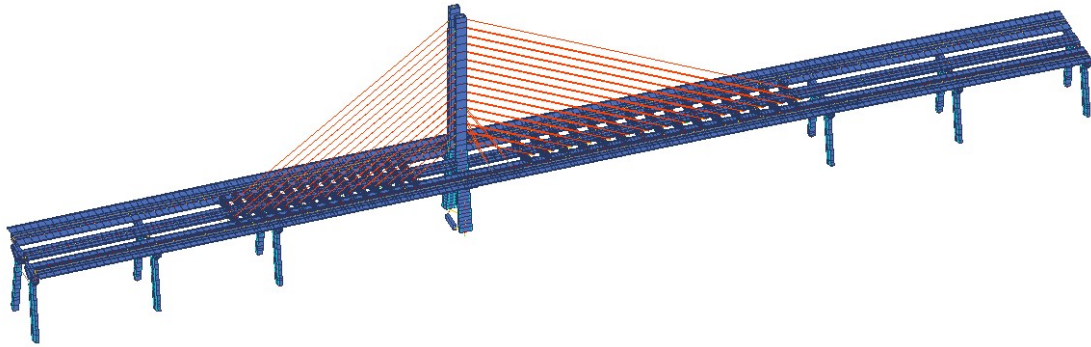


Figure 8, Model of the Cable-Stayed Bridge

These two cases were enveloped to compute the seismic forces for design of the entire cable-stayed bridge. The design obtained through this simplified analysis was verified using time history analysis as described below.

TIME HISTORY ANALYSIS

The design of the entire bridge was verified using time history analysis considering the following effects:

- Non-synchronous ground motions due to wave passage effects, site effects, and incoherence. Displacement ground motions were applied in three perpendicular directions.
- Soil-structure interaction was considered with nonlinear response soil and depth-variable ground motions.
- Liquefaction and lateral spreading of the soils surrounding the main tower foundation of the cable-stayed bridge.
- The analysis was geometrically nonlinear (P-delta effects).

Modeling

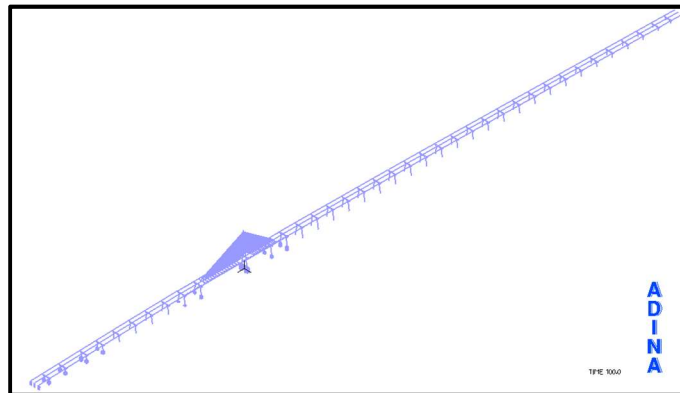


Figure 9, ADINA model of the entire bridge, including the cable-stayed bridge and the east and west approaches

The time history analysis of the bridge was performed using ADINA [11]. The model used is shown in Figure 9. The cable-stayed bridge model is shown in close-up in Figure 10. The model includes detailed models of the pile supported foundations (Piers W02, W01, MST, and E01). These include discrete models of each pile and support from inelastic P_y , T_z , and Q_u springs. The spread footing at Pier E02 was modeled using discrete springs to allow rocking (if it were to occur).

The model of the east approach is shown in Figure 11. For the pile foundations at piers E07-E10, depth varying ground motions were applied through non-linear soil springs. For spread footing foundations, the foundation stiffness was represented in the model with impedance matrixes. Similar modeling was used for the west approach, which includes only spread footings.

Global Response

Figure 12 shows the calculated pier drifts in the longitudinal direction for the 2475-year event. It may be seen that within the east and west approaches, the fixed piers exhibit much larger drifts than do other piers—though the maximum drift of 45 mm is very small relative to the pier height—approximately 45 m at Pier W05 (the units in all plots are kN and m). This is consistent with the fact that the fixed piers support all the longitudinal seismic forces (friction in the bearings was neglected) whereas “sliding” piers only need to support their own weight. It may also be observed that the drifts tend to increase with

pier height towards the cable stayed bridge, which is also sensible (note that the main tower of the cable-stayed bridge is not included in this plot of typical piers).

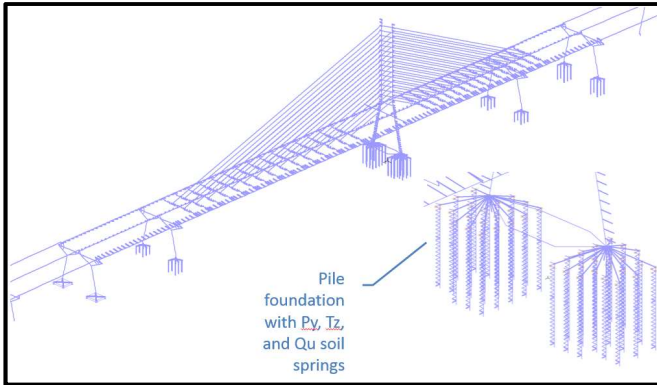


Figure 10, ADINA model of the cable-stayed bridge

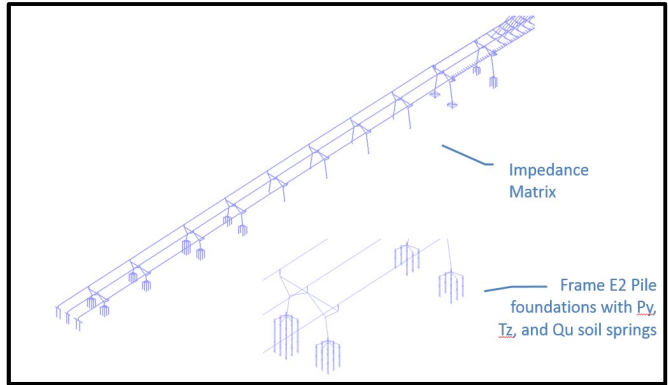


Figure 11, ADINA model of the east approach

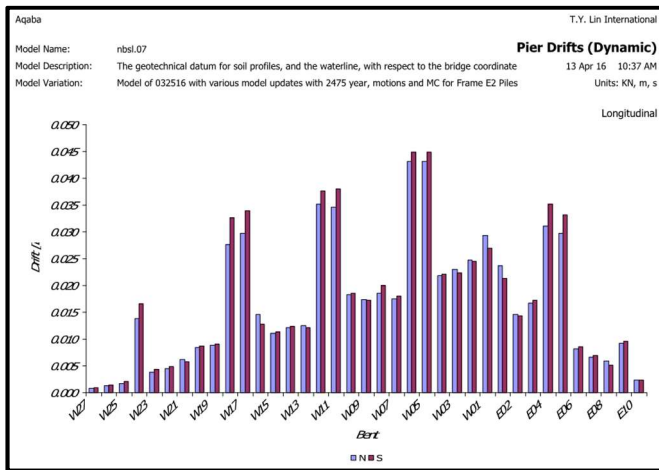


Figure 12, Longitudinal pier drifts, 2475-event

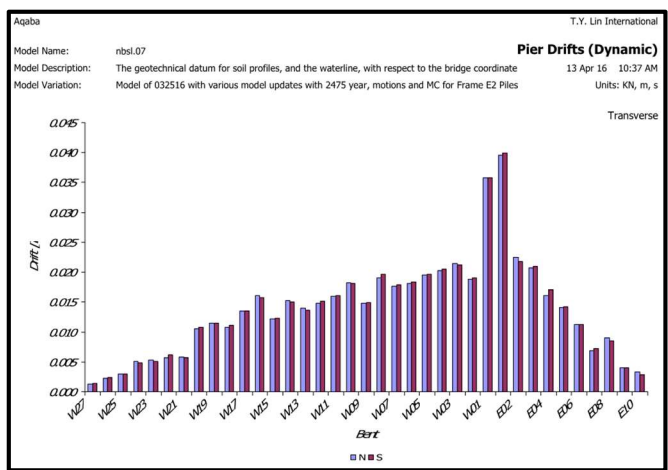


Figure 13, Transverse pier drifts, 2475-year event

Figure 13 shows the calculated pier drifts in the transverse direction, also for the 2475-year event. The same trend of increasing drifts with pier height is seen in this direction also, with Piers W01 and E01—one either side of the main tower of the cable-stayed bridge—being outliers from the general trend. Relative to other piers—of similar height—these piers react to a significant portion of the mass of the cable-stayed bridge. They also react to a larger tributary length of structure than do the other piers (they react to the lateral inertia of the cable-stayed bridge without supporting the corresponding vertical weight, which is supported by the stays).

Lateral Spreading Analysis of the Main Span Tower Foundation

Figure 14 shows the maximum bending moments in the piles for the 2475-year event, for non-liquefied conditions. It shows the pile moment in each of the two halves of the foundation (under the north and south tower legs) as a function of depth below the top of pile cap. The values plotted are the maximum at each depth over five independent ground motions. The pile response is assumed elastic, although the soil springs (Py, Tz, & Qu) are inelastic. The maximum bending moments occur at the soffit of the pile cap, as expected.

Figure 15 shows the pile maximum bending moments considering lateral spreading. Depth-variable motions were applied including the ground displacement that occurs through lateral spreading. A typical motion of the ground surface at the north pod of the MST foundation is shown in Figure 16. The motion is applied to the pile cap and piles through nonlinear P-y springs that represent the liquefied stiffness of the soil. The lateral spreading is resisted by the pile cap and piles, with the result that the bending moments in the piles are much higher than for the non-liquefied case. This is the governing case for pile flexure.

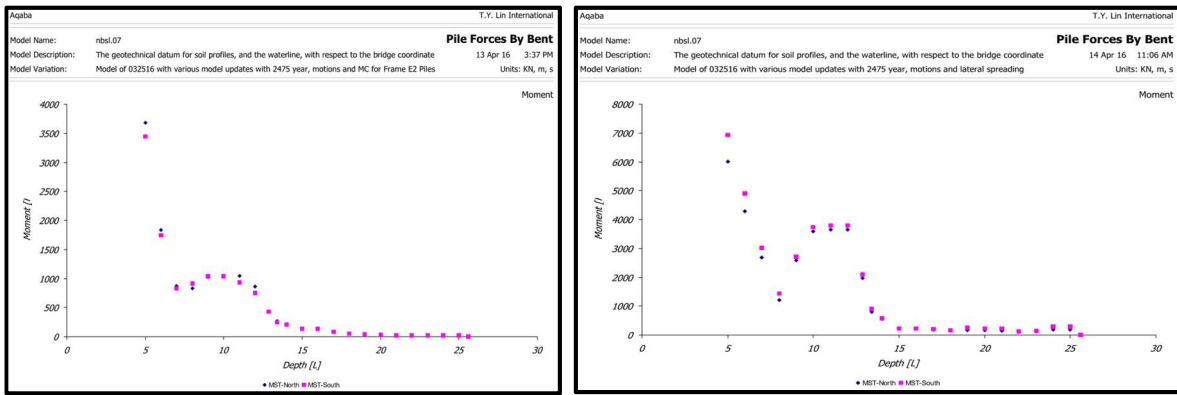


Figure 14, Bending moments in MST piles, non-liquefied case. Figure 15, Bending moments in MST piles, liquefied case

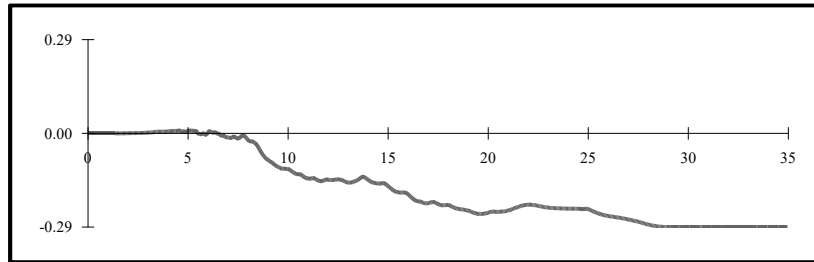


Figure 16, Ground motion due to lateral spreading at MST-north

The same analysis approach was used for the foundation of Pier E01.

CONCLUSIONS

The seismic design of the New Champlain Bridge has been carried out in accordance with the governing codes and using state-of-the-art techniques. For the cable-stayed bridge and adjacent bents, however, it was found that seismic loads were generally not controlling the lateral design. For the most part, wind loads were the controlling loading. This is not surprising given the modest seismicity of the site, the adoption of a lighter and more flexible steel superstructure with steel pier caps which helped to mitigate against seismic forces, the large size of the structure and the high-level crossing of the bridge which exposes the structure to more significant wind forces. Nevertheless, seismic hazards, including risk of soil liquefaction were integrated with special considerations and advance analyses by the Engineers in the design of this major structure.

REFERENCES

- [1] Thenhaus, K.W., Campbell, N., Gupta, Smith, D.F., and Khater, M.M, 2012, A Consistent Cross-Border Seismic Hazard Model for Loss Estimation and Risk Management in Canada, 15th World Conference on Earthquake Engineering, Lisbon.
- [2] Atkinson, G. (2009) " Earthquake Time Histories Compatible with the 2005 National Building Code of Canada Uniform Hazard Spectrum," Canadian Journal of Civil Engineering, 2009, 36(6): 991-1000.
- [3] (REI) Risk Engineering, Inc. (2001), "Technical Basis for Revision of Regulatory Guidance on Design Ground Motions: Hazard- and Risk-consistent Ground Motion Spectra Guidelines NUREG/CR-6728," Prepared for the Division of Engineering Technology Office of Nuclear Regulatory Research, U.S. Nuclear Regulatory Commission.
- [4] Abrahamson, N. A. (2007), "Hard-Rock Coherency Functions Based on the Pinyon Flat Array Data," Electric Power Research Institute, Draft Report, July 2007.
- [5] Itasca (2011), "Fast Lagrangian Analysis of Continua, FLAC" Itasca Consulting Group, User's manual, Minneapolis
- [6] Beaty, M., and Byrne, P.M., (1998). "An Effective Stress Model for Predicting Liquefaction Behavior of Sand," Proc. of a Specialty Conference, Geotechnical Earthquake Engineering and Soil Dynamics, ASCE pp. 766-777, Seattle.
- [7] New Bridge for the Saint Lawrence Corridor Project, *Project Agreement between The Minister of Public Works and Government Services and Signature of the Saint Laurent Group*.
- [8] New Champlain Bridge Corridor Project: *Design Basis Report*, June 17, 2016.
- [9] Standards Council of Canada, Canadian Highway Bridge Design Code, CAN/CSA-S6 including supplement No.1
- [10] Bentley Systems, RM Bridge Advanced version V8i.08.11.18.01.
- [11] ADINA R&D, ADINA version 8.7.